Doctoral degree thesis

Development of TX-816 and its derivatives as 5-Aminolevurinic acid-based photodynamic therapy sensitizer

（5-アミノレブリン酸を用いた光線力学療法増感剤としての TX-816 及びその誘導体の開発）

2021, March

Doctoral Course 3rd, Biological Science and Technology, Life and Materials Systems Engineering,

Graduate School of Advanced Technology and Science, Tokushima University

篠原　侑成

Contents

Chapter 1. Development of TX-816, a novel Schiff-base derivative, for enhancing effect of 5-aminolevurinic acid-based photodynamic therapy

Chapter 2. Development of 4-alkylaniline derivative UTX-122-128 with improved hydrolyzability of TX-816

Chapter 1. Development of TX-816, a novel Schiff-base derivative, for enhancing effect of 5-aminolevurinic acid-based photodynamic therapy

1 Abstract

5-Aminolevulinic acid (ALA), a precursor of protoporphyrin IX (PpIX), is now widely used for photodynamic therapy (ALA-PDT) of various cancers. Recently, I found that treatment of cancer cells with the Schiff base derivative TX-816 along with ALA could significantly increase the efficacy of ALA-PDT. This enhancing effect of TX-816 on ALA-PDT is attributed to 3,5-dichlorosalicylaldehyde (DCSA), a molecule produced by the degradation of TX-816. Similar to TX-816, DCSA significantly enhances the effect of ALA-PDT. Furthermore, DCSA could restore the sensitivity of cancer cells that acquired resistance to ALA-PDT. These results indicate that DCSA, as well as TX-816, is a potent lead compound for the development of an ALA-PDT sensitizer.

2 Introduction

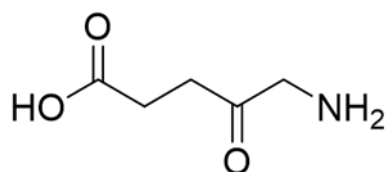**5-Aminolevulinic acid（ALA）**

Fig. 1　Structure of ALA

ALA (Fig. 1) is one of the natural amino acids and is known to act as a precursor of porphyrin *in vivo*. Porphyrins biosynthesized from ALA are extremely important co-factors in animal and plant cells [1]. In particular, metal porphyrins in which some metal ions are coordinated at the center of porphyrins have various functions. For example, magnesium ion-coordinated porphyrins are important co-factors of plant chlorophyll and play a central role in photosynthesis. In addition, iron (II) porphyrin called Heme is used as a co-factor of hemoglobin, myoglobin, cytochrome P450 and catalase [2-4]. Heme plays an extremely important role in the body. After being synthesized *in vivo*, ALA is rapidly converted to porphyrins. Therefore, ALA production step is the most important in the porphyrin biosynthesis. Also ALA has high water solubility and low cytotoxicity, so it can be widely applied as a drug, supplement or reagent. In fact, ALA is already used in the medical field. As ALA is known to polymerize under basic conditions, it is generally used in the form of hydrochloride or phosphate.

Photodynamic Therapy：PDT

PDT is a treatment method in which an administered photosensitizer is accumulated in tumor tissue or new blood vessels, and then the tissue is irradiated with laser light to cause a photochemical reaction to degenerate and necrotize cells. This denaturation and necrosis are due to the strong oxidative action of singlet oxygen, which is a type of reactive oxygen species (ROS) produced by the reaction of laser light of a specific wavelength with a photosensitive substance.

The life of ROS generated by PDT is extremely short, about 0.04-4 μs. The laser used in PDT is

different from the high-power laser used in general laser treatment so that we hardly feel the heat. The major feature is that the output is weak and the range in which the reaction occurs can be controlled only at the lesion site where the photosensitizer has accumulated. Therefore, PDT is expected to develop in various disease areas as a lesion site-selective treatment method that is less invasive to normal tissues [5].

Production of PpIX via metabolism from ALA

ALA is converted to Protoporphyrin IX (PpIX) by undergoing the following metabolism *in vivo* (Fig. 2) [6].

1. ALA dehydratase condenses two molecules of ALA to produce porphobilinogen (PBG).

2. Porphovirinogen deaminase produces linear hydroxymethylpyran (HMB) from four molecules of porphobilinogen.

3. Uroporphyrinogen III synthase forms the prototype of the porphyrin ring, which is accompanied by the inversion of one pyrrole ring to produce uroporphyrinogen III.

4. Uroporphyrinogen decarboxylase desorbs four molecules of CO_2 from uroporphyrinogen III to produce coproporphyrinogen III.

5. Coproporphyrinogen oxidase desorbs two molecules of CO_2 to produce protoporphyrinogen IX.

6. Finally, protoporphyrinogen oxidase oxidizes protoporphyrinogen IX to produce PpIX. At this time, a compound having properties as a photosensitizer is obtained only when the porphyrinogen is changed to a porphyrin ring. The intermediate porphyrinogen is neither a fluorescent substance nor a photosensitizer.
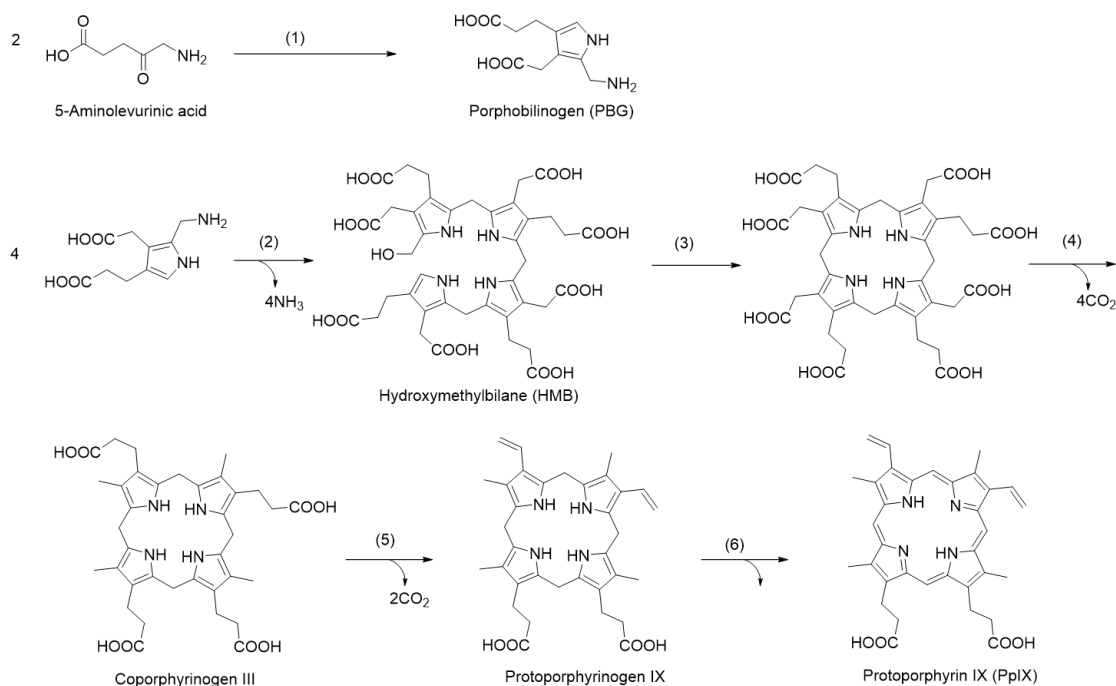
Fig. 2 Biosynthesis pathway of Protoporphyrin IX in cells

ALA-based photodynamic therapy （ALA-PDT）

Photodynamic diagnosis (ALA-PDD) and photodynamic therapy (ALA-PDT) using ALA are widely used as diagnostic and therapeutic methods for various cancers [8,14]. The exogenous ALA is taken up into cells by PEPT1, a proton-coupled oligopeptide transporter, that is a solute carrier family 15 member A1 (SLC15A1) [9]. After 8 molecules of ALA are metabolized to protoporphyrin IX (PpIX) in the cytoplasm and mitochondria through the above 6-step steps. Subsequently, PpIX is coordinated with iron (II) by ferrokiratase and metabolized to Heme, and then metabolized to bilirubin. The bilirubin is rapidly released extracellularly by the ABCC transporter. It is known that PpIX accumulation hardly occurs in normal cells. On the other hand, PpIX accumulation in tumor cells is thought to occur selectively due to the following three causes (Fig. 3) [10].

① Iron concentration in tumor cells: It has been pointed out that the iron concentration in tumor cells is low. Although PpIX is produced, less iron should be inserted compared to normal cell.

② Expression level of transporter that takes 5-ALA into the cell: In general, compounds such as drugs are taken up and excreted into the cell via the transporter expressed on the cell membrane. 5-ALA is taken up into cells by PEPT1, and it is known that the amount of PpIX accumulation is proportion to

expression level of PEPT1.

③ Expression level of transporter that excretes PpIX: PpIX produced from 5-ALA is excreted by ABCG2 transporter which is one of the drug excretion transporters. It is known that the amount of PpIX accumulation is inversely proportion to expression level of ABCG2.

Due to these factors, PpIX selectively accumulates in tumor cells.
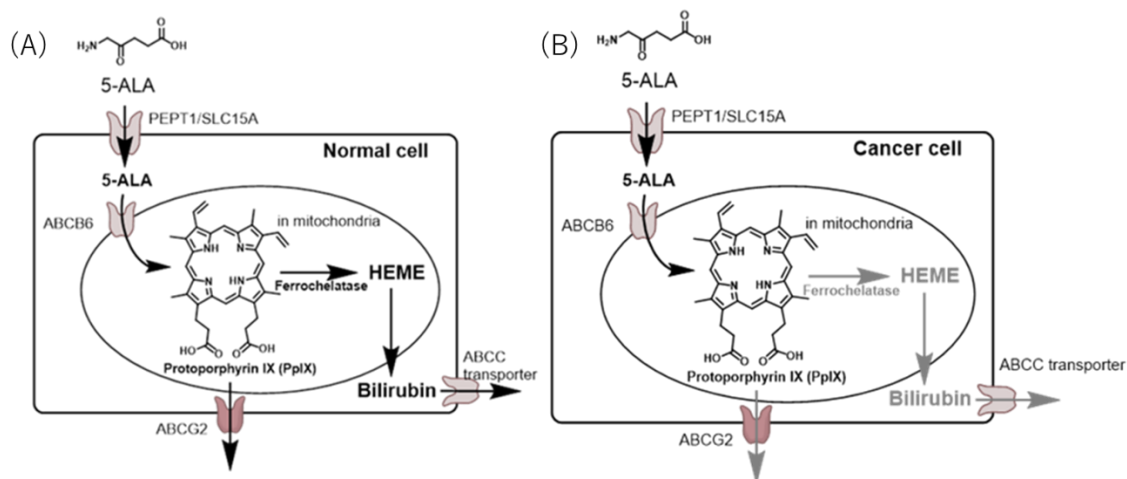

Fig. 3 The mechanism of selective ALA-PDT to treat cancer cells (A) Normal cells, (B) Cancer cells
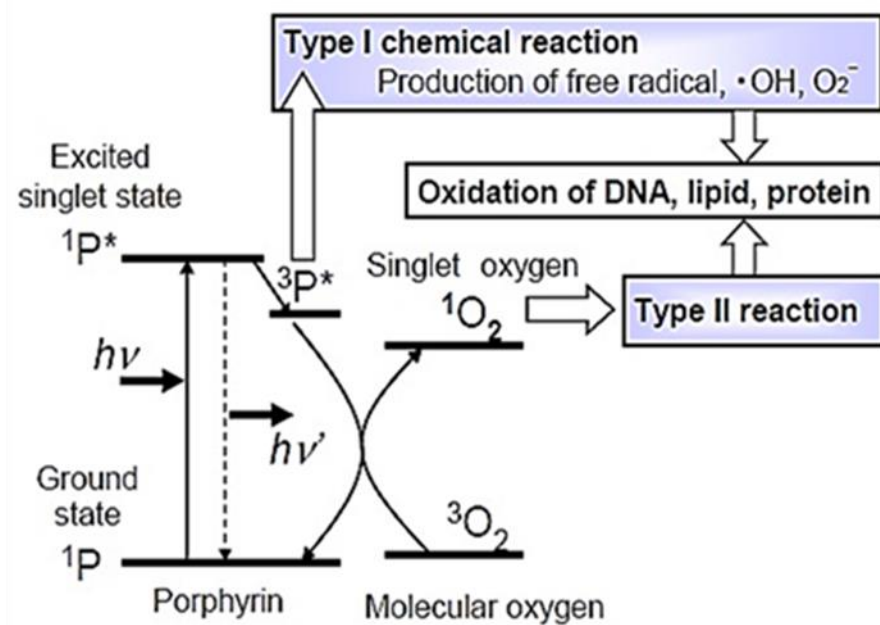

Fig. 4 Production of reactive oxygen species (ROS) from PpIX

Here, when tumor cells are irradiated with blue visible light at 405 nm-410 nm, the accumulated PpIX emits red fluorescence at 635 nm, so that the tumor tissue can be efficiently visualized (ALA-PDD).   ALA-

PDD is also used for tumor resection in the medical field. Furthermore, when irradiated with red visible light having a wavelength longer than 630 nm, PpIX absorbs this wavelength and induces cell death by generating ROS from PpIX (ALA-PDT). As a result, a therapeutic effect can be expected in various tumor cells. ALA-PDT has been successfully treated for patients suffering from neoplastic or non-neoplastic diseases (Fig. 4).

In recent studies, tumor cell selectivity in ALA-PDT is demonstrated by the balance between 5-ALA influx via transporters such as PEPT1 and intracellular PpIX release via ABC transporters such as ABCG2 [10-13]. It was found that the cell-killing effect of ALA-PDT was reduced in tumor cells with low PEPT1 expression and tumor cells with high ABCG2 expression.

Therefore, I considered a method of using 5-ALA in combination with other compounds as a method for improving the cytocidal effect of ALA-PDT. By screening from our chemical library, I was able to discover *N*-3', 5'-dichloro-2'-hydroxybenzylidene-2-chloro-4-nitroaniline (TX-816) having a Schiff base. (Fig.5A). When 5-ALA and TX-816 were used in combination, the amount of intracellular PpIX accumulation was increased as compared with ALA alone, and the cytocidal effect of ALA-PDT was improved accordingly.
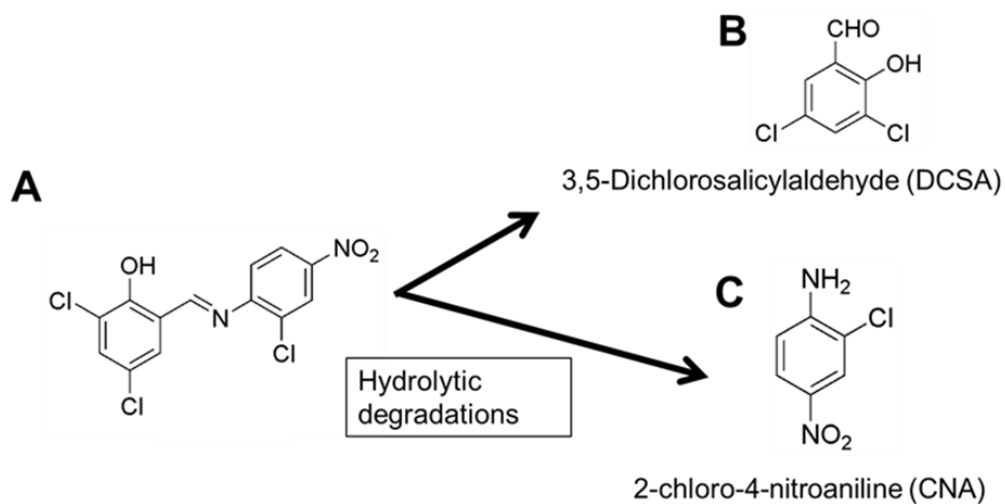

Fig. 5 Chemical structures of TX-816 (A) and its degradation products, DCSA (B) and CNA (C)

3 Materials and Methods

3.1 Materials

All solvents and chemicals were purchased from Wako Pure Chemical Industries (Osaka, Japan), Tokyo Chemical Industries (Tokyo, Japan), and Sigma-Aldrich (St. Louis, MO, USA). In the chemical synthesis, progress of reactions was monitored using Merck silica gel 60 F_{254} TLC plates (Merck, Darmstadt, Germany) with EtOAc/n-Hexane. Column Chromatography was performed using silica-gel 60N purchased from Kanto Chemical (Tokyo, Japan). ^{1}H-NMR spectra was recorded using JNM-EX-400 (JEOL, Tokyo, Japan) in deutrated solvent. Date are reported as follows: chemical shift, multiplicity (s = singlet, d = doublet, t = triplet, q = quartet, dd = double doublet, m = multiplet, brs = broad singlet), coupling constants (Hz), and integration. Broad singlet peaks, speculated to arise from OH protons, are also noted. Purity of all final compounds was confirmed at >95% using high performance liquid chromatography (HPLC) (JASCO PU-2089 Plus and JASCO MD-2018 Plus : JASCO Corporation, Tokyo, Japan) on a TSKgel Amide-80 3 μm column (4.6 mm I.D.×15 cm). The elutes were n-Hexane(A) and $CHCl_3$(B). The conditions for analytical HPLC as follows: flow rate 0.5 mL/min, detection wavelength 330 nm, gradient A/B 0-15 min (100/0 to 30/70), 15-30 min (30/70), 30-40 (30/70 to 0/100), 40-45 min (0/100), 45-50 min (0/100 to 100/0). Column temperature was not controlled. High-resolution mass spectroscopy (HRMS) was performed using a Waters LCT Premier XE (Waters, Massachusetts, America) and Waters ACQUITY UPLC (Waters, Massachusetts, America). TX-816 produces DCSA and CNA by hydrolytic degradation in the solvent. Hematoporphyrin IX dihydrochloride (HEMP) and dipyridamole (DPM) were purchased from Wako Pure Chemical Industries (Osaka, Japan), whereas DCSA and CNA were purchased from Tokyo Chemical Industry (Tokyo, Japan).

3.2 Synthesis of TX-816

DCSA (504 mg, 2.64 mmol) was dissolved in dry toluene (30 mL). CNA (683 mg, 3.96 mmol, 1.5 eq.) was added to the solution on ice-bath. The reaction mixture was warmed up to room temperature and refluxed for 24 h using Dean-Stark apparatus. After the reaction, the solvent was evaporated. The residue was purified by flash silica-gel column chromatography using EtOAc/n-Hexane. TX-816 was afforded as red solid; yield 29% (266 mg, 0.77 mmol). ^{1}H-NMR (400 MHz, DMSO-d6) δ 13.5 (br s, 1H), 9.14 (s, 1H), 8.48 (d, J = 2.4 Hz, 1H), 8.38 (dd, J = 8.8, 2.4 Hz, 1H), 7.87 (d, J = 2.4 Hz, 1H), 7.84 (s, 1H), 7.82 (d, J = 2.8 Hz, 1H), TOF-ESI-MS m/z: Calculated for: $C_{13}H_8N_2O_3Cl_3^+$: 344.9601, Found: 344.9617 ($[M + H]^+$). HPLC (t_R =19.1 min).
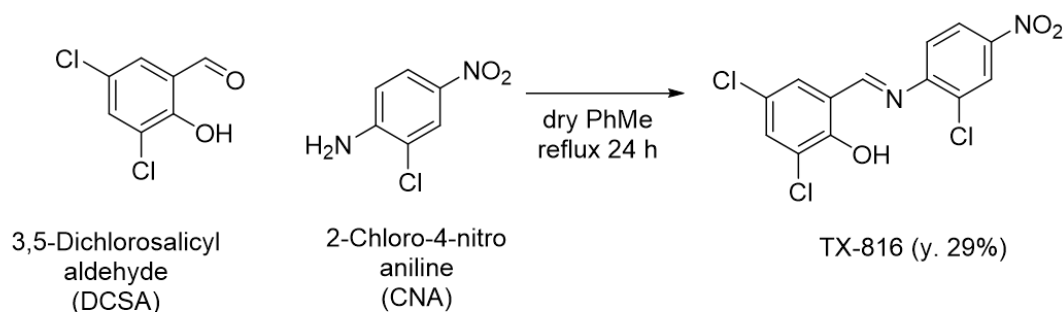
Scheme 1. Synthesis of TX-816

3.3 Cells and cell culture

The poorly differentiated gastric cancer cell line MKN-45 was kindly provided by Dr. Suzuki (Fukushima Medical College, Fukushima, Japan). The human gastric cancer cell line KKLS, which was established from a metastasized lymph node of a patient with multiple metastasis in the liver and lymph nodes, was kindly provided by Dr. Mai (Cancer Research Institute of Kanazawa University) [15]. The poorly differentiated signet ring cell carcinoma cell line NUGC-4 was obtained from the Japanese Cancer Research Resources Bank (Tokyo, Japan).

Cells were maintained in RPMI-1640 medium supplemented with 10% (v/v) heat-inactivated fetal bovine serum and 50 µg/mL kanamycin at 37°C in a humidified atmosphere containing 5% CO_2.

3.4 ALA-PDT sensitivity assay by LED irradiation

Cells were seeded at a density of 5×10^3 cells/well in a 96-well plate and cultured at 37°C in 5% CO2 for 24 h. Test compounds such as TX-816, DCSA, CNA, and DPM were dissolved in DMSO and added to the culture medium at the stated concentrations. The final concentration of DMSO in the culture medium was 0.5%. Thereafter, serial dilutions of ALA were added to the culture medium at concentrations between 7.8 and 1,000 µM. After 4 h of incubation, the medium was replaced by fresh complete medium and the 96-well plate was exposed to LED irradiation (630 nm, 80 mW/cm^2) emitted by an LED irradiation unit provided by SBI ALA PROMO (Tokyo, Japan) for 5 min (Fig. 6). The LED light spot was an equally illuminated rectangular spot measuring 128×86 mm in size covering the whole area of the 96-well culture plate.
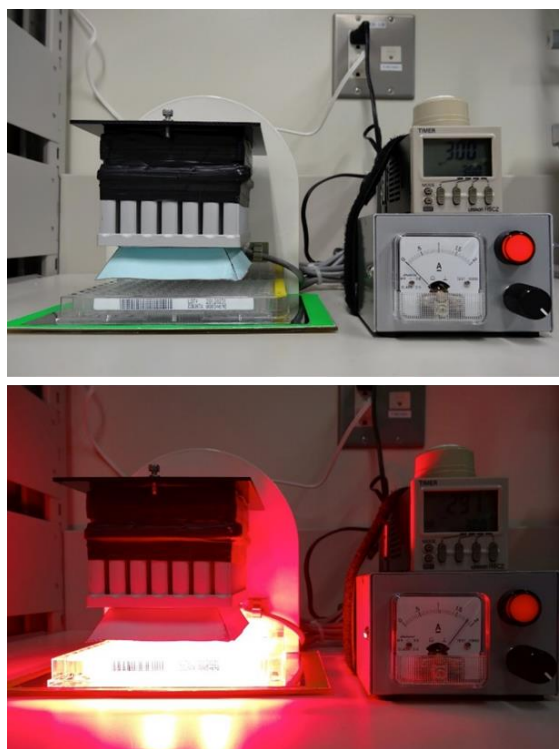

Fig. 6 The LED light source. The LED irradiation unit equips four module boards consisting of twenty (4 × 5) LEDs.

After LED irradiation, cells were further incubated for 48 – 72 h, and cell viability was measured by a colorimetric assay using Cell Counting Kit-8 (Dojindo Laboratories, Kumamoto, Japan) according to the

manufacturer's instructions. After 72 h of incubation, the medium was replaced by fresh medium containing the WST-8 reagent. After 3 h, absorbance in each well was measured at 450 nm (with a reference wavelength of 620 nm) using a microplate spectrophotometer, ImmunoMini NJ-2300 (BioTec, Tokyo, Japan, Tokyo, Japan).

The percentage of cell growth inhibition was calculated by applying the following formula:

$$\text{cell growth inhibition (\%)} = \left(1 - \frac{T}{C}\right) \times 100$$

, where C and T are the mean absorbance values of the control and treated groups, respectively. The IC_{50} value was determined graphically from the dose–response curve with at least three drug concentration points.

3.5   The isobologram method with 5-ALA and TX-816

The isobologram method [16] was used to determine whether the effect of TX-816 on ALA-PDT sensitivity was additive, synergistic, or competitive. In the combination assay, serial dilutions of TX-816 (0, 6.25, 12.5, 25, 50, 100, and 200 μM) were added to the culture medium. On the other hand, ALA was added at concentrations of 0, 6.25, 12.5, 25, 50, and 100 μM. After 4 h of incubation, the medium was replaced by fresh complete medium, and the 96-well plate was exposed to LED irradiation for 5 min. Cell viability was measured by a colorimetric assay as stated above. The IC_{10}, IC_{20}, IC_{30}, IC_{40}, and IC_{50} values of ALA alone and TX-816 alone were determined graphically from the dose–response curve. The IC_{10}, IC_{20}, IC_{30}, IC_{40}, and IC_{50} values of ALA were defined as a_1, a_2, a_3, a_4, a_5 and those of TX-816 were defined as b_1, b_2, b_3, b_4, b_5, respectively. At first, $(0, a_5)$ and $(b_5, 0)$ were plotted on the Y axis and X axis of the graph, respectively. Next, (b_5-b_1, a_1), (b_5-b_2, a_2), (b_5-b_3, a_3), (b_5-b_4, a_4), (b_1, a_5-a_1), (b_2, a_5-a_2), (b_3, a_5-a_3), (b_4, a_5-a_4) were plotted on the graph. Finally, the IC_{50} values of the combinations of ALA and TX-816 were represented on the graph. The inner area surrounded by the two lines of their IC_{10} - IC_{50} values shows the range of predictive IC_{50} values whose corresponding combinations have an additive effect; IC_{50} values of the combination treatments located within the gray zone, under the gray zone, and above the gray zone correspond to combinations having additive, synergistic, and competitive effects, respectively (Fig.7, Drug A as ALA and Drug B as TX-816).
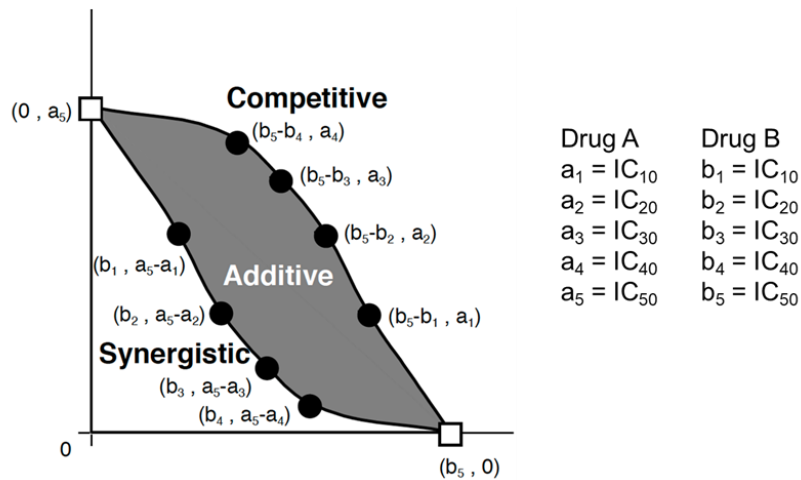
Fig. 7 The isobologram analysis of the combination treatment with Drug A and Drug B. Each area is Additive, Synergistic and Competitive.

3.6 Establishment of ALA-PDT-resistant MKN-45 cells

Resistant cells were established by repeated treatment with ALA-PDT and sub-cloning, as shown in Fig. 8. Briefly, MKN-45 cells were seeded into a 35-mm dish and incubated with 200 μM ALA for 4 h. The cells were exposed to red LED light (630 nm) for 5 min. The surviving and re-growing cells, which were resistant to ALA, were collected and seeded into a new dish, treated again with ALA-PDT, and re-seeded into a new 15-cm dish after each treatment.

Fig. 8 Establishment of MKN-45 cells with acquired resistance to ALA-PDT. To obtain cell lines resistant to ALA-PDT, MKN-45 cells were treated repeatedly with ALA-PDT and resistant cell colonies were isolated and cultured separately (R1, R2, and R13). Clone R13 was subject to re-cloning and subsequently, R13-1 and R13-2 were isolated.

3.7 Measurement of intracellular PpIX

Cells (2×10^6 cells) were seeded in 6-cm dishes and incubated for 24 h. TX-816, DCSA, and DPM were added to the medium at the stated concentrations bef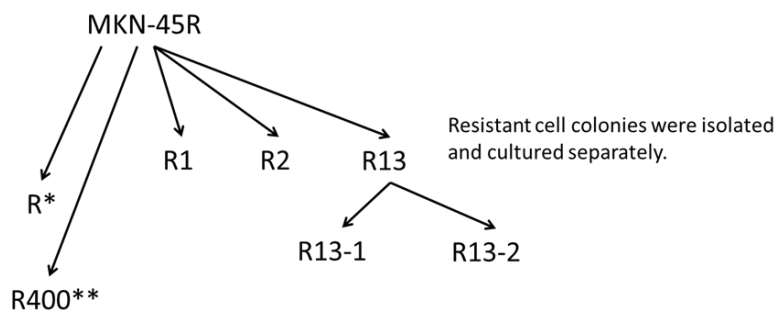ore ALA addition. After 4 h of incubation, cells were harvested using 2 mL of 0.25% Trypsin-1 mM EDTA. A cell suspension was collected in a 5-mL tube and centrifuged at 800 rpm for 5 min. The supernatant was removed with aspirator and cells were washed with phosphate-buffered saline. Finally, the cell pellet was suspended in 500 µL of 2.5% Triton X-100 solution and the cell suspension was transferred into a 0.5-mL micro tube, vortexed, incubated for 5 min at room temperature, and centrifuged at 15,000 rpm for 10 min. The fluorescence intensity of PpIX in the supernatant was measured using a SEC2000-UV/VIS spectrophotometer (excitation: 410 nm, emission: 630 nm).

3.8 Reverse transcription-polymerase chain reaction (RT-PCR) analysis of mRNA expression of PEPT1 and ABCG2

Total RNA was extracted from cells using ISOGEN (Nippon Gene, Tokyo, Japan) according to the manufacturer's protocol. First-strand cDNA was prepared from total RNA via reverse transcriptase reaction using ReverTra Ace (TOYOBO, Osaka, Japan). Next, cDNA was amplified by PCR in a Thermal Cycler Dice (TaKaRa Bio, Otsu, Japan). The specific sense and antisense primers were as follows: 5'-TGACGCCAATTCTCGGAGCTCTTATC-3' (sense) and 5'-CAGGAACATCACCCTCGTAACCATCT-3' (anti-sense) for PEPT1 (NM_005073, SLC15A1) (the product size: 665 bp); 5'-GGTTACGTGGTACAAGATGATGTTGTGATG-3' (sense) and 5'-CCAGCTCTGTTCTGGATTCCAGTAGAATCA-3' (anti-sense) for ABCG2 (NM_004827) (the product size: 920 bp); and 5'-GAAAATCTGGCACCACACCTT-3' (sense) and 5'-TTGAAGGTAGTTTCGTGGAT-3'(anti-sense) for β-actin (NM_001101) (the product size: 519 bp), used as the internal control. The PCR reaction consisted of hot-start incubation at 95°C for 3 min and 33 cycles, each consisting of 30 s at 94°C, 40 s at 62°C, and 60 s at 72°C. The resulting amplicons were separated by 1.2% agarose gel electrophoresis and detected with ethidium bromide under ultraviolet light.

4   Results

4.1   The enhancing effects of TX-816 on ALA-PDT

The IC_{50} of combination with TX-816 and ALA was declined following as increasing concentration of TX-816 (10 to 30 µM). The Schiff base derivative TX-816 improved the sensitizing effect of ALA-PDT on MKN-45 cells in a dose-dependent manner (Fig. 9).
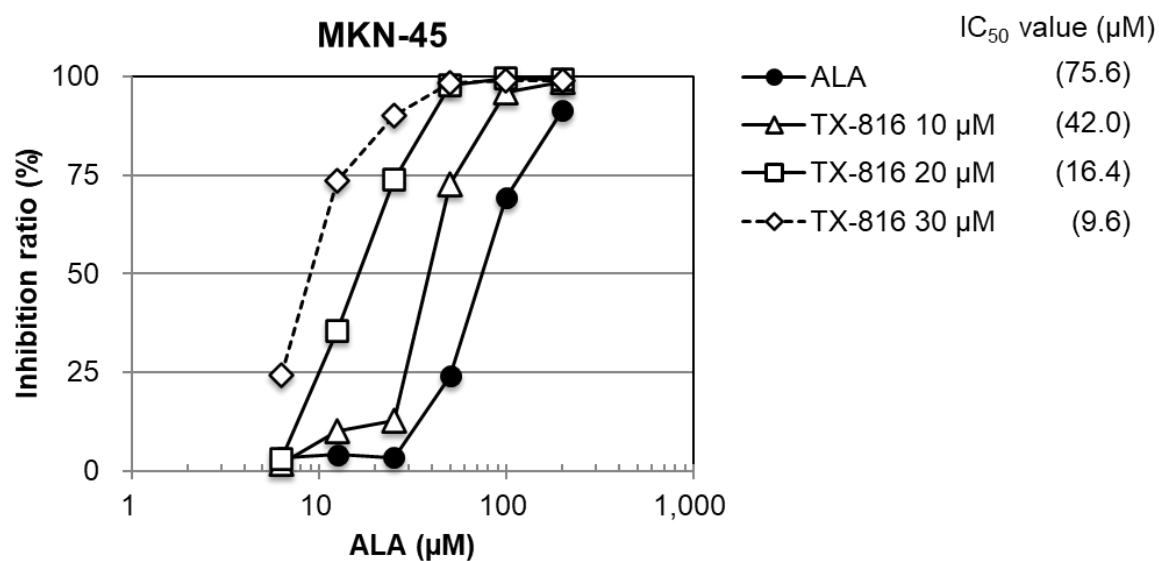

Fig. 9   The enhancing effect of TX-816 on ALA-PDT. MKN-45 cells were seeded at a density of 5×10^3 cells/well in a 96-well plate. After 24 h of incubation, TX-816 (5, 10, or 20 µM) was added to the culture medium.

Isobologram analysis revealed that the plot of combined with TX-816 and ALA-PDT was placed in synergistic area, and that combination had a synergistic effect on MKN-45 cells (Fig. 10).
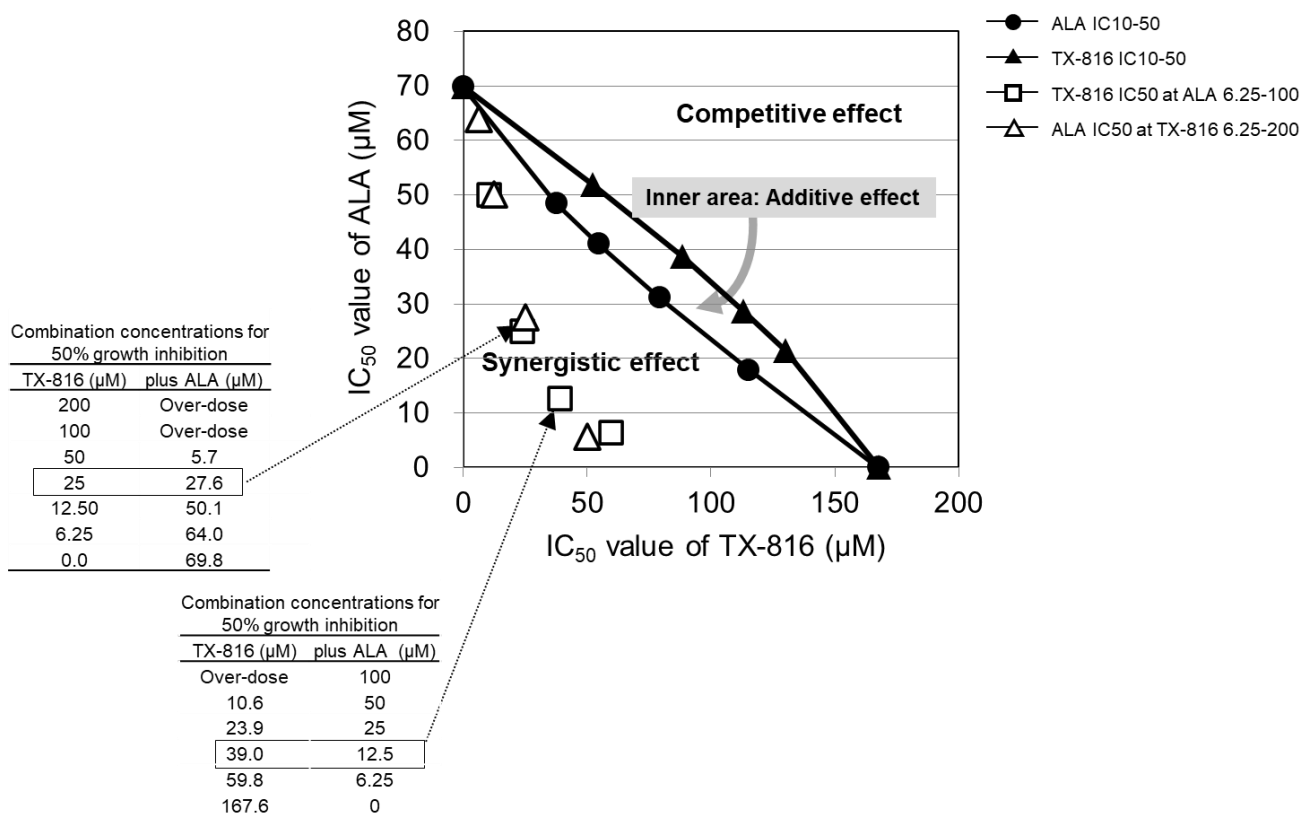
Fig. 10. The isobologram analysis of the combination treatment with ALA and TX-816. Various concentrations of TX-816 and ALA were added to the culture medium as described in the "Materials and methods" section. The IC_{50} values of the combination treatments were determined by the colorimetric assay using the WST-8 reagent, and the type of the effect was evaluated by the isobologram analysis. The IC_{50} values of ALA and TX-816 combinations are represented by open triangles ($\triangle$) and open squares ($\square$). The inner area surrounded by the two lines shows the range of predictive IC_{50} values if the combinations have an additive effect. Since the IC_{50} values are located in the low-concentration side under the gray zone, these combinations were judged to have synergistic effects.

14

4.2 The enhancing effects of TX-816 and DCSA, which is TX-816 degradation product, on ALA-PDT

I found that TX-816 was hydrolyzed by DCSA and CNA in the solvent (Fig. 5). Therefore, the sensitizing effect of ALA-PDT was measured when each DCSA and CNA were used in combination. Only DCSA significantly improved the sensitizing effect of ALA-PDT on MKN-45 cells, human gastric cancer cells. Also, the sensitizing effect of DCSA in combination was almost equivalent to that of TX-816 in combination. On the other hand, when CNA was used in combination, the sensitizing effect of ALA-PDT was reduced (Fig. 11). It was suggested that the active center of TX-816 is DCSA.
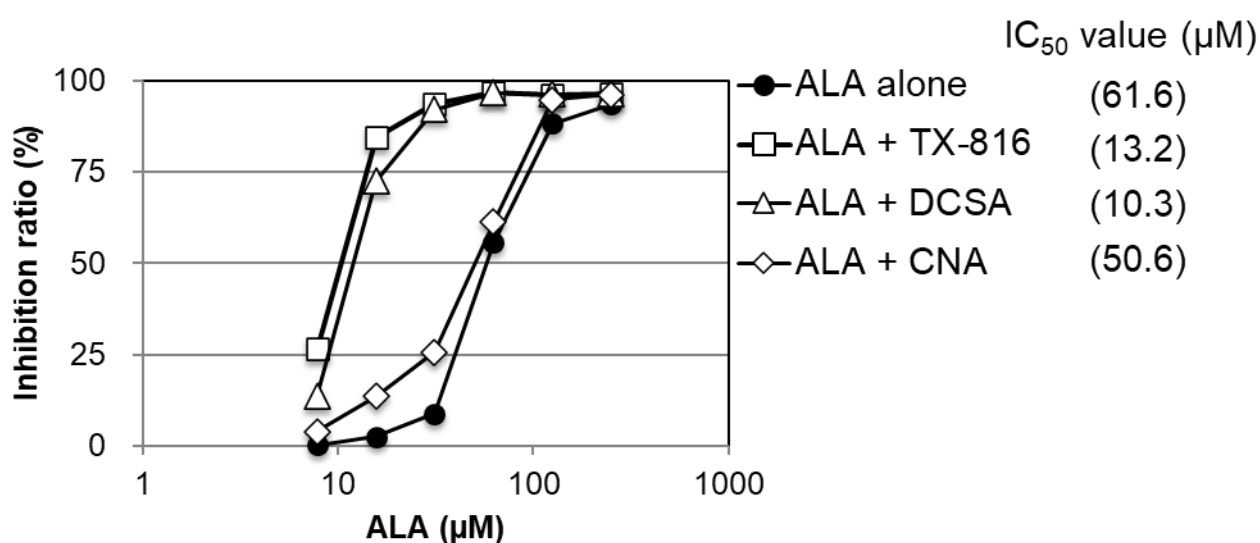

Fig. 11   The enhancing effects of TX-816, DCSA, and CNA on ALA-PDT against MKN-45 cells. MKN-45 cells were seeded at a density of 5×10^3 cells/well in a 96-well plate. After 24 h of incubation, TX-816, DCSA, or CNA (20 µM) was added to the culture medium.

4.3 The ALA-PDT-enhancing effects of TX-816, DCSA, and DPM in parental MKN-45 cells and its ALA-PDT resistant cell lines

All resistant cells were parental to MKN-45 cells, and these resistant cells were also resistant to 1 mM ALA. Among the four types of resistant cells, the expression level of PEPT1 transporter mRNA was reduced and the expression level of ABCG2 transporter mRNA was improved in R1 cells. However, in other resistant cells (R cells, R13 cells, R400 cells), the expression level of PEPT1 transporter mRNA was similar to that of MKN-45 cells, but the expression of ABCG2 transporter mRNA was not observed. (Fig.12A). Although DCSA was able to recover the sensitivity of the ALA-PDT resistant cell lines R, R13, and R400, R1 cells remained highly resistant to ALA-PDT even after the combination treatment with ALA and DCSA (Fig. 12B). The sensitizing effect on resistant cells was almost the same in the DCSA combination group as in the TX-816 combination group (Table 1).

DPM, a platelet inhibitor and coronary vasodilator used to prevent arterial thromboembolism, is known to inhibit ABCG2 and equilibration nucleoside transporters such as SLC29A1 and SLC29A2. DPM increased the sensitivity of ALA-PDT in tumor cells expressing both PEPT1 and ABCG2, however it did not improve the sensitivity to ALA-PDT resistant cells differentiated from MKN-45 cells. KKLS cells, human gastric cancer cells, have lower mRNA expression levels of PEPT1 and ABCG2 than MKN-45 cells. In KKLS cells, the sensitizing effect on ALA-PDT was improved only when DCSA was used in combination with a high concentration of ALA. The IC_{50} value for KKLS cells was 505.1 µM with ALA alone, 336.9 µM with DCSA and ALA, and 829.4 µM with DPM and ALA. However, in NUGC-4 cells expressing both PEPT1 and ABCG2, the sensitizing effect of ALA-PDT was improved in both DCSA combination group and DPM combination group. These IC_{50} values in NUGC-4 cells were 3244 µM with ALA alone, 125.7 µM with DCSA and ALA, and 171.4 µM with DPM and ALA.
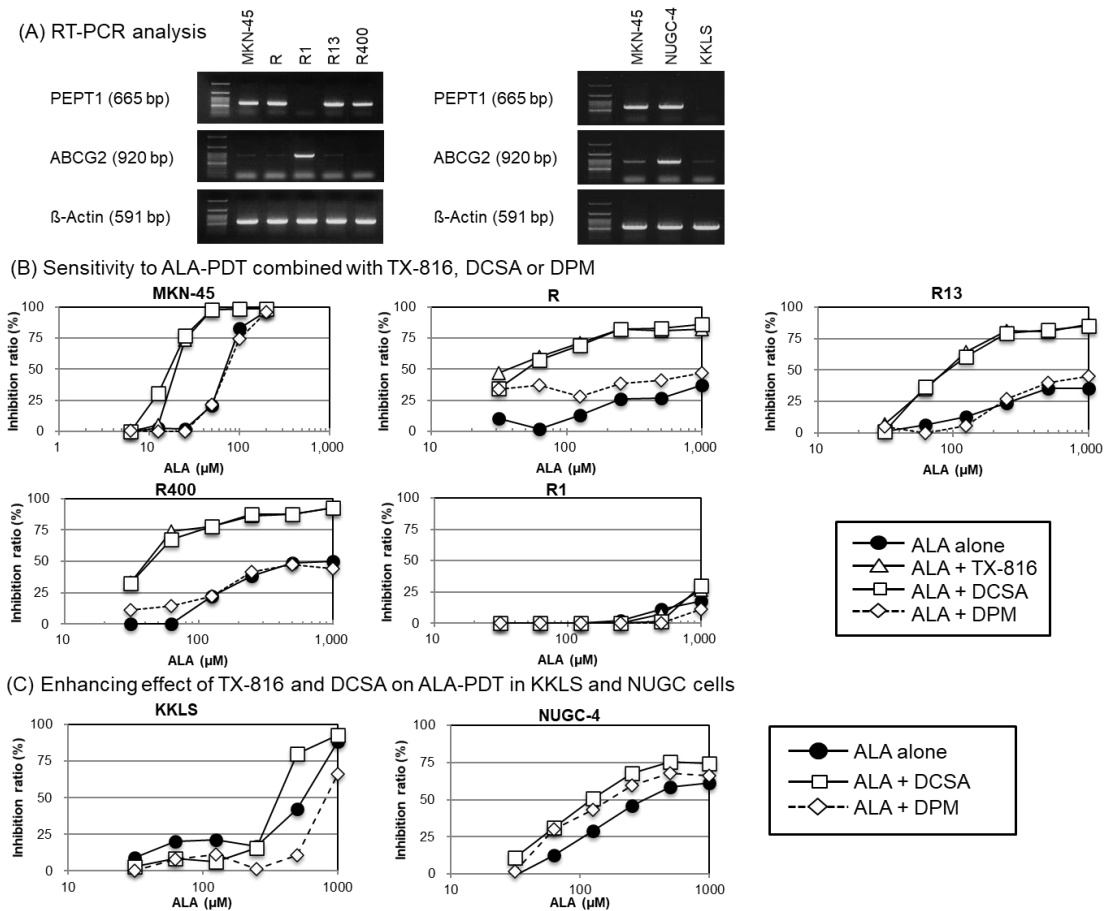
Fig. 12   The ALA-PDT enhancing effects of TX-816, DCSA, and DPM in parental MKN-45 cells, its ALA-PDT-resistant cell lines, KKLS cells, and NUGC cells. (A) RT-PCR analysis of PEPT1 and ABCG2 in gastric cancer cells. (B) The enhancing effects of TX-816, DCSA, and DPM on ALA-PDT in ALA-PDT-resistant cell lines. (C) The enhancing effects of DCSA and DPM on ALA-PDT in KKLS and NUGC cells. Cells were seeded at a density of 5×10^3 cells/well in a 96-well plate. After 24 h of incubation, TX-816, DCSA (20 µM), or DPM (10 µM) was added to the culture medium.

Table 1. The enhancing effects of TX-816, DCSA and DPM on ALA-PDT in ALA-PDT-resistant cell lines.

| | IC_{50} (µM) of ALA | | | |
| | | Combination with ALA | | |
	ALA	TX-816	DCSA	DPM
MKN-45	64.3	21.9	17.0	77.0
R	>1000	35.9	54.4	>1000
R1	>1000	>1000	>1000	>1000
R13	>1000	96.3	102.4	>1000
R400	>1000	41.5	46.7	>1000

On the other hand, the DCSA combination group did not show a sensitizing effect on either MKN-45 cells or ALA-PDT resistant cells in PDT (HEMP-PDT) using HEMP. HEMP-PDT, a single agent of HEMP, showed high sensitivity in all cell types. The IC_{50} value is as follows (Fig. 13).

- MKN-45 cells: 5.7 µM in HEMP monotherapy group, 5.3 µM in DCSA combination group

- R cells: 7.5 µM for HEMP therapy group, 8.2 µM for DCSA combination group

- R13 cells: 7.5 µM in HEMP therapy group, 7.5 µM in DCSA combination group

- R1 cells: 7.6 µM in HEMP therapy group, 8.1 µM in DCSA combination group

These results suggested that DCSA did not activate the cytocidal effect of PpIX mediated by ROS production.
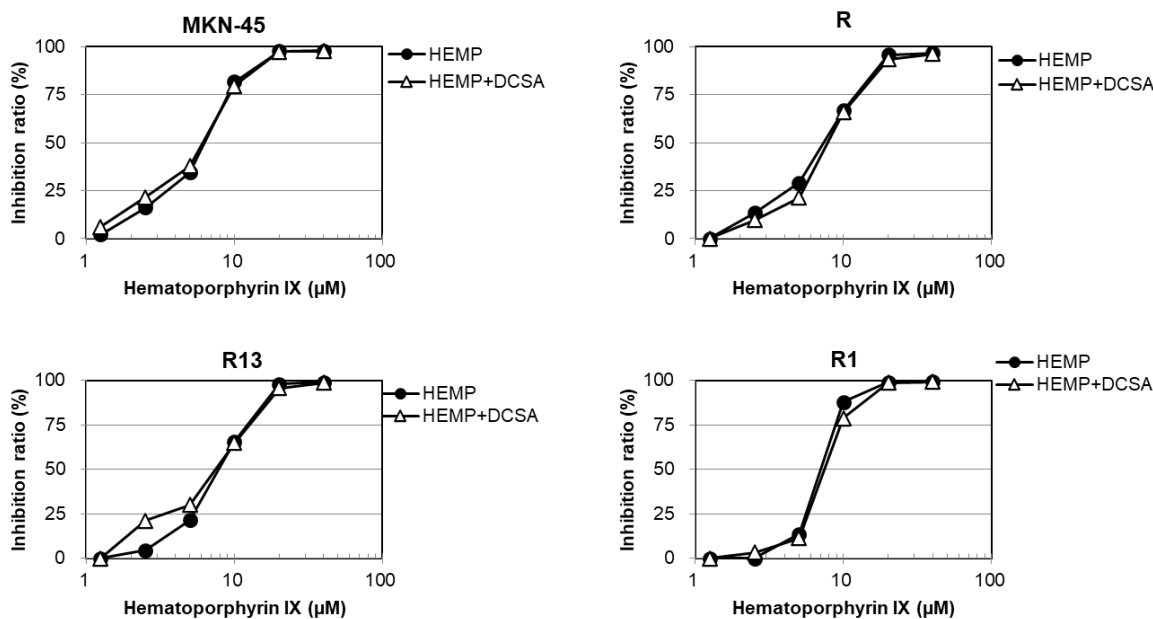
Fig. 13 The effect of DCSA on HEMP-PDT in parental MKN-45 and its derived ALA-PDT-resistant cell lines. MKN-45 and its ALA-PDT-resistant cells were seeded at a density of 5×10^3 cells/well in a 96-well plate. After 24 h of incubation, DCSA (20 μM) was added to the culture medium. Then, serial dilutions of HEMP were added to the culture medium at concentrations of 1.25 – 40 μM. After 4 h of incubation, the 96-well plate was exposed to LED irradiation for 5 min and further incubated for 72 h.

4.4 Increased intracellular accumulation of PpIX after the combination treatment with ALA and DCSA.

The amount of intracellular PpIX accumulated after 4 hours of ALA treatment was reduced in all resistant cells (Fig. 14). In particular, the intracellular PpIX amount of R13 cells treated with ALA 100 μM alone was less than about 10% as compared with the parent strain MKN-45 cells. However, the combined treatment with DCSA improved the accumulation of intracellular PpIX in MKN-45 cells and various resistant cells (Fig. 15). When treated with ALA 100 μM and DCSA 20 μM, the accumulation of intracellular PpIX in MKN-45 cells was 2.1 times that of the single agent, and that of R13 cells was 4.8 times (Table 2).
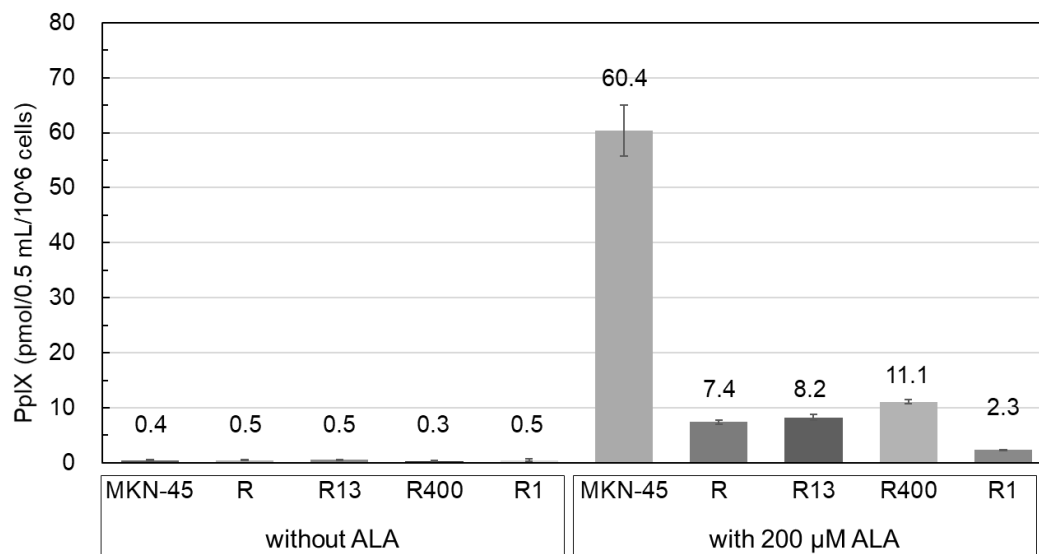
19

Fig. 14. Decreased intracellular accumulation of PpIX in highly ALA-PDT-resistant cells.
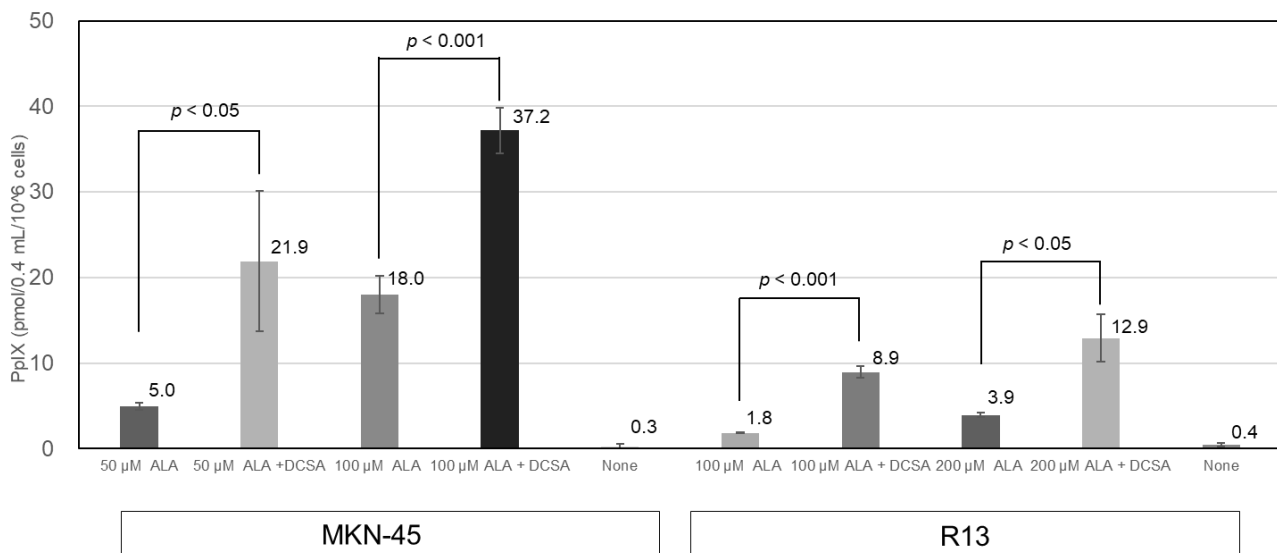

Fig. 15. Increased intracellular accumulation of PpIX in MKN-45 and R13 cells after combination treatment with ALA and DCSA.

Table 2. Intracellular accumulation of PpIX in MKN-45 and R13 cells after combination treatment with ALA and DCSA. *NT: not tested.

	MKN45 PpIX (pmol/0.5 mL/10^6 cells)			R13 PpIX (pmol/0.5 mL/10^6 cells)		
	ALA alone	ALA + 20 μM DCSA	T/C ratio	ALA alone	ALA + 20 μM DCSA	T/C ratio
ALA 50 μM	5.0	21.9	4.4	NT*	NT	
ALA 100 μM	18.0	37.2	2.1	1.8	8.9	4.8
ALA 200 μM	NT	NT		3.9	12.9	3.3
None	0.3	NT		0.4	NT	

5. Discussion

In this study, I found that the Schiff base derivative TX-816 significantly improved the sensitizing effect of ALA-PDT by significantly increasing the accumulation of intracellular PpIX. Furthermore, the sensitizing effect of TX-816 in ALA-PDT was due to DCSA generation with hydrolysis of TX-816. When TX-816 or DCSA were used together, the overall mechanism of ALA-PDT sensitization effect has not yet been clarified. However, DCSA did not improve the sensitization effect in HEMP-PDT. ALA-PDT resistant cells differentiated from the parent strains MKN-45 cells and MKN-45 cells were highly sensitive to HEMP-PDT. These findings suggested that DCSA did not directly activate the cytocidal activity of PpIX by ROS production.

The expression level of PEPT1 mRNA was extremely low in R1 cells. R1 cells did not take up ALA until the cytocidal activity was exhibited in ALA-PDT. As a result, the sensitizing effect of DCSA was not shown. On the other hand, although the expression level of PEPT1 mRNA was increased and the expression level of ABCG2 mRNA was decreased in R cells, R13 cells and R400 cells, the intracellular PpIX accumulation after ALA treatment against these resistant cells was reduced compared to MKN-45 cells. The ABCB6 transporter located in mitochondrial membrane is known to function as a coproporphyrin III (CP III) specific transporter [17]. ABCB6 is also known to be present in cell membranes [18]. Previously, Matsumoto K. *et al*. reported that ABCB6 expressed on the cell membrane releases CPIII extracellularly and that function was found to be upregulated in a hypoxia [19]. Since the hypoxic environment significantly reduced ALA-derived PpIX accumulation in tumor cells [20,21], functional expression of ABCB6 on plasma membrane is an important factor in PpIX accumulation after ALA treatment.

To elucidate the molecular mechanism of ALA-PDT resistance, I investigated the gene expression profile in resistant cells by microarray analysis. The results showed the gene expression profile of the Heme metabolic pathway and iron reduction system in the resistant cells, as well as a wide variety of ALA influx and PpIX outflow transporters. The expression level of ABCB6 mRNA is high in R1 cells, and ABCB6 may be one of the target molecules that confer ALA-PDT resistance to cells. However, there was almost no difference in the expression level of ABCB6 mRNA between R cells, R13 cells and MKN-45 cells. R cells and R13 cells have high expression levels of ABC transporters such as ABCA3, ABCB4, ABCG4, ABCC2, and ABCC3. ABCC2 and ABCC3 transporters function in biliary transport of bilirubin glucuronides and contribute to multidrug resistance to vinblastine, methotrexate and VP16 [22-24]. It was found that the expression levels of Ferrochelatase and Heme Oxygenase were increased in all these resistant cell types including R1 cells. It was suggested that activation of Heme metabolic pathway may be an important mechanism for tumor cells to acquire ALA-PDT resistance. Further research is needed to clarify the relationship between the sensitizing effect on ALA-PDT of DCSA and the function of these ABC transporters. The ABCG2 transporter was found not to be a molecular target for DCSA in MKN-45 cells. It was because that the expression level of ABCG2 mRNA is low in MKN-45 cells, it showed almost no sensitivity to DPM which is an ABCG2 inhibitor, and the sensitizing effect of ALA-PDT was improved when DCSA is used in combination.

6. Conclusion

In this chapter, TX-816 enhanced the sensitizing effect of ALA-PDT on MKN-45 cell in a dose-dependent manner, and its effect was synergistic with isobologram analysis. DCSA, the active center of TX-816, improved the sensitizing effect of ALA-PDT on MKN-45 cell and ALA-PDT resistant cells. DCSA was increased the accumulation of intracellular PpIX in its cell lines. DCSA was found to be a useful lead compound for the development of ALA-PDT sensitizers, and TX-816 was found to be useful as a compound for designing ALA-PDT sensitizer prodrugs [25].

Chapter 2. Development of 4-alkylaniline derivative UTX-122-128 with improved hydrolyzability of TX-816

1. Abstract

5-Aminolevulinic acid (ALA), a precursor of protoporphyrin IX (PpIX), is now widely used for photodynamic therapy (ALA-PDT) of various cancers. In chapter 1, I found that treatment of cancer cells with the Schiff base derivative TX-816 along with ALA could significantly increase the efficacy of ALA-PDT. These results indicate that DCSA, as well as TX-816, is a potent lead compound for the development of an ALA-PDT sensitizer. DSCA, conferred ALA-PDT sensitizing effect in TX-816, may be considered to law stability in blood for aldehyde group. UTX-122-128, TX-816 derivatives with CNA replaced by 4-alkylaniline, showed higher ALA-PDT effects than DCSA, and these were more stable than TX-816 in solvent. The accumulation of intracellular PpIX with these derivatives were increasing compared with DCSA. DCSA-derivatives UTX-122-128 might be useful compounds for designing prodrug-type ALA-PDT sensitizers.

2. Introduction

In chapter 1, I found that the Schiff base derivative *N*-3',5'-dichloro-2'-hydroxybenzylidene-2-chloro-4-nitroaniline, TX-816, could significantly increase the effect of ALA-PDT by accelerating intracellular PpIX accumulation [25]. However, TX-816 was unstable in the aqueous solution and was so quickly hydrolyzed into 3,5-Dichlorosalicylaldehyde (DCSA) and 2-Chloro-4-nitroaniline (CNA). Therefore, I looked for searched the method to give the hydrolysis resistance which to TX-816 was obtained the hydrolysis resistance derivatives. Herein, I report the enhanced cytocidal activity of ALA-PDT against human cancer cells using novel derivatives of TX-816.

3. Materials and Methods

3.1 Materials

All solvents and chemicals were purchased from Wako Pure Chemical Industries (Osaka, Japan), Tokyo Chemical Industries (Tokyo, Japan), and Sigma-Aldrich (St. Louis, MO, USA). In the chemical synthesis, progress of reactions was monitored using Merck silica gel 60 F_{254} TLC plates (Merck, Darmstadt, Germany) with EtOAc/n-Hexane. Column Chromatography was performed using silica-gel 60N purchased from Kanto Chemical (Tokyo, Japan). ^{1}H-NMR spectra was recorded using JNM-EX-400 (JEOL, Tokyo, Japan) in deutrated solvent. Dates are reported as follows: chemical shift, multiplicity (s = singlet, d = doublet, t = triplet, q = quartet, dd = double doublet, m = multiplet, brs = broad singlet), coupling constants (Hz), and integration. Broad singlet peaks, speculated to arise from OH protons, are also noted. Purity of all final compounds was confirmed at >95% using high performance liquid chromatography (HPLC) (JASCO PU-2089 Plus and JASCO MD-2018 Plus : JASCO Corporation, Tokyo, Japan) on a TSKgel Amide-80 3 μm column (4.6 mm I.D.×15 cm). The elutes were n-Hexane(A) and $CHCl_3$(B). The conditions for analytical HPLC as follows: flow rate 0.5 mL/min, detection wavelength 330 nm, gradient A/B 0-15 min (100/0 to 30/70), 15-30 min (30/70), 30-40 (30/70 to 0/100), 40-45 min (0/100), 45-50 min (0/100 to 100/0). Column temperature was not controlled. High-resolution mass spectroscopy (HRMS) was performed using a Waters LCT Premier XE (Waters, Massachusetts, America) and Waters ACQUITY UPLC (Waters, Massachusetts, America).

3.2 Synthesis of UTX-122 to UTX-128 which were substituted 4-alkylaniline derivatives from CNA

General method : DCSA + 4-alkylanilines (Compound 1 to 7 ; UTX-122 to UTX-128)

4-Alkylaniline (1.0 - 1.5 equiv.) and dried 3A molecular sieves were mixed with DCSA (1.0 equiv.) dissolved in dry toluene under N_2 gas on ice-bath. The reaction mixture was warmed up to room temperature and refluxed for 2 – 5 h. After the evaporation, the oily residue was purified by flash silica-gel column chromatography using EtOAc/n-Hexane.[26] Novel TX-816 derivatives substituted CNA to 4-Alkylaniline (Carbon Chain 0-6) were synthesized to inflict hydrolysis resistance to their Schiff-base compounds.

1. Compound **1** (UTX-122)

General method using Aniline (220 μL, 2.40 mmol) afforded as an orange solid; yield 98% (415 mg, 1.56 mmol). ^{1}H-NMR (400 MHz, DMSO-D6) δ 9.01 (d, J = 3.6 Hz, 1H), 7.69-7.73 (m, 2H), 7.46-7.48 (m, 4H), 7.33-7.36 (m, 1H), TOF-ESI-MS m/z: Calculated for $C_{13}H_{10}NOCl_2^+$: 266.0139, Found: 266.0152 ([M + H]$^+$). HPLC (t_R =13.3 min).

2. Compound **2** (UTX-123)

General method using p-Toluidine (186 mg, 1.74 mmol) afforded as an orange solid; yield 94% (418 mg, 1.49 mmol). ^{1}H-NMR (400 MHz, DMSO-d6) δ 14.7 (br s, 1H), 9.02 (s, 1H), 7.72 (d, J = 2.4 Hz, 1H), 7.70 (d, J = 2.8 Hz, 1H), 7.40 (d, J = 8.8 Hz, 2H), 7.30 (d, J = 8.0 Hz, 2H), 2.34 (s, 3H), TOF-ESI-MS m/z: Calculated for $C_{14}H_{12}NOCl_2^+$: 280.0296, Found: 280.0298 ([M + H]$^+$). HPLC (t_R =13.8 min).

3. Compound **3** (UTX-124)

General method using 4-Ethylaniline (400 μL, 3.20 mmol) afforded as an orange solid; yield 95% (729 mg, 2.48 mmol). ^{1}H-NMR (400 MHz, DMSO-d6) δ 9.01 (s, 1H), 7.71 (d, J = 2.8 Hz, 1H), 7.69 (d, J = 2.0 Hz, 1H), 7.40 (d, J = 8.8 Hz, 2H), 7.32 (d, J = 8.4 Hz, 2H), 2.63 (dd, J = 7.6 Hz, 2H), 1.18 (t, J = 7.6, 7.6 Hz, 3H), TOF-ESI-MS m/z: Calculated for $C_{15}H_{14}NOCl_2^+$: 294.0452, Found: 294.0439 ([M + H]$^+$). HPLC (t_R =13.6 min).

4. Compound **4** (UTX-125)

General method using 4-Propylaniline (231 μL, 1.57 mmol) afforded as an orange solid; yield 100% (324 mg, 1.05 mmol). ^{1}H-NMR (400 MHz, DMSO-d6) δ 9.01 (s, 1H), 7.71 (d, J = 1.6 Hz, 1H), 7.69 (d, J = 1.6

Hz, 1H), 7.40 (d, J = 8.4 Hz, 2H), 7.30 (d, J = 8.0 Hz, 2H), 2.58 (t, J = 7.6, 7.6 Hz, 2H), 1.54-1.63 (m, 2H), 0.88 (t, J = 7.4, 7.4 Hz, 3H), TOF-ESI-MS m/z: Calculated for $C_{16}H_{16}NOCl_2^+$: 308.0609, Found: 308.0613 ([M + H]$^+$). HPLC (t_R =13.8 min).

5. Compound **5** (UTX-126)

General method using 4-Butylaniline (415 µL, 2.62 mmol) afforded as an orange solid; yield 95% (804 mg, 2.50 mmol). ^{1}H-NMR (400 MHz, DMSO-d6) δ 14.7 (br s, 1H), 9.02 (s, 1H), 7.72 (d, J = 2.8 Hz, 1H), 7.70 (d, J = 2.4 Hz, 1H), 7.41 (d, J = 8.0 Hz, 2H), 7.31 (d, J = 8.0 Hz, 2H), 2.63 (t, J = 9.2, 9.2 Hz, 2H), 1.53-1.60 (m, 2H), 1.26-1.35 (m, 2H), 0.90 (t, J = 7.6 Hz, 3H), TOF-ESI-MS m/z: Calculated for $C_{17}H_{18}NOCl_2^+$: 322.0765, Found: 322.0750 ([M + H]$^+$). HPLC (t_R =13.2 min).

6. Compound **6** (UTX-127)

General method using 4-Pentylaniline (185 µL, 1.05 mmol) afforded as an orange solid; yield 97% (343 mg, 1.02 mmol). ^{1}H-NMR (400 MHz, DMSO-d6) δ 9.01 (s, 1H), 7.70 (d, J = 8.0 Hz, 2H), 7.40 (d, J = 6.8 Hz, 2H), 7.30 (d, J = 7.6 Hz, 2H), 2.59 (t, J = 7.6, 7.6 Hz, 2H), 1.53-1.60 (m, 2H), 1.27-1.30 (m, 4H), 0.84 (t, J = 6.2, 6.2 Hz, 3H), TOF-ESI-MS m/z: Calculated for $C_{18}H_{20}NOCl_2^+$: 336.0922, Found: 336.0938 ([M + H]$^+$). HPLC (t_R =13.1 min).

7. Compound **7** (UTX-128)

General method using p-Hexylaniline (400 µL, 2.09 mmol) afforded as an orange solid; yield 47% (430 mg, 1.23 mmol). ^{1}H-NMR (400 MHz, DMSO-d6) δ 14.7 (br s, 1H), 9.01 (s, 1H), 7.71(d, J =2.8 Hz, 1H), 7.69 (d, J = 2.8 Hz, 1H), 7.39 (d, J = 8.4 Hz, 2H), 7.29 (d, J = 8.4 Hz, 2H), 2.59 (t, J = 7.8, 7.8 Hz, 2H), 1.52-1.57 (m, 2H), 1.23-1.29 (m, 6H), 0.83 (t, J = 7.0, 7.0 Hz, 3H), TOF-ESI-MS m/z: Calculated for $C_{19}H_{22}NOCl_2^+$: 350.1078, Found: 350.1067 ([M + H]$^+$). HPLC (t_R =12.7 min).
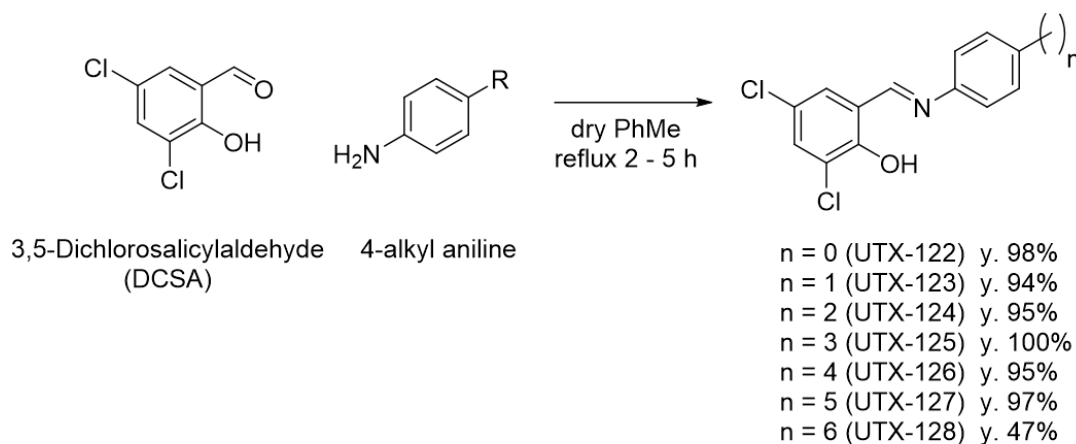
Scheme 2. Synthesis of DCSA-derivatives UTX-122 to UTX-128

3.3 Cells and cell culture

The poorly differentiated gastric cancer cell line MKN-45 was kindly provided by Dr. Suzuki (Fukushima Medical College, Fukushima, Japan). The human gastric cancer cell line KKLS, which was established from a metastasized lymph node of a patient with multiple metastasis in the liver and lymph nodes, was kindly provided by Dr. Mai (Cancer Research Institute of Kanazawa University) [15]. The poorly differentiated signet ring cell carcinoma cell line NUGC-4 was obtained from the Japanese Cancer Research Resources Bank (Tokyo, Japan).

Cells were maintained in RPMI-1640 medium supplemented with 10% (v/v) heat-inactivated fetal bovine serum and 50 μg/mL kanamycin at 37°C in a humidified atmosphere containing 5% CO_2.

3.4 ALA-PDT sensitivity assay by LED irradiation

Cells were seeded at a density of 5×10^3 cells/well in a 96-well plate and cultured at 37°C in 5% CO2 for 24 h. Test compounds such as UTX-122 to UTX-128 were dissolved in DMSO and added to the culture medium at the stated concentrations. The final concentration of DMSO in the culture medium was 0.5%. Thereafter, serial dilutions of ALA were added to the culture medium at concentrations between 7.8 and 1,000 μM. After 4 h of incubation, the medium was replaced by fresh complete medium and the 96-well plate was

exposed to LED irradiation (630 nm, 80 mW/cm^2) emitted by an LED irradiation unit provided by SBI ALA PROMO (Tokyo, Japan) for 5 min. The LED light spot was an equally illuminated rectangular spot measuring 128 × 86 mm in size covering the whole area of the 96-well culture plate.

After LED irradiation, cells were further incubated for 48 – 72 h, and cell viability was measured by a colorimetric assay using Cell Counting Kit-8 (Dojindo Laboratories, Kumamoto, Japan) according to the manufacturer's instructions. After 72 h of incubation, the medium was replaced by fresh medium containing the WST-8 reagent. After 3 h, absorbance in each well was measured at 450 nm (with a reference wavelength of 620 nm) using a microplate spectrophotometer, ImmunoMini NJ-2300 (BioTec, Tokyo, Japan, Tokyo, Japan).

The percentage of cell growth inhibition was calculated by applying the following formula:

$$\text{cell growth inhibition (\%)} = \left(1 - \frac{T}{C}\right) \times 100$$

, where C and T are the mean absorbance values of the control and treated groups, respectively. The IC$_{50}$ value was determined graphically from the dose–response curve with at least three drug concentration points.

3.5   Evaluation of chemical stability by GC/MS

The stability of UTX-122 to UTX-128, 4-alkylaniline derivatives, and TX-816 was evaluated by a gas chromatography-mass spectrometry (GC/MS) using Agilent 7820A GC system coupled to Agilent 5977E MSD system (Agilent Technologies, CA, USA). 1,5-Diphenyl-1,4-pentadien-3-one as an internal control was dissolved in DMSO or 10% water/90% DMSO at 1.2 mM. The samples tested were dissolved at concentrations from 5 to 10 mM with the solvent including an internal control and were immediately sonicated for 5 min. Then, the sample solutions were filtrated with syringe filter (Minisart Syringe Filter, 0.2 µm, Sartorius AG, Göttingen, Deutschland) and settled at room temperature until measurement by GC/MS analysis. After appropriate incubation time, an aliquot of the sample solution was separated by GC system and all peaks corresponding to each compound including an internal control were identified by ion-fragment pattern based on a single quadrupole mass spectrometer with an electrospray ionization source (ESI). Separation was achieved with Ultra Inert Columns HP-5ms capillary GC column (30 m × 0.25 mm, 0.25 µm) (Agilent Technologies).

Chromatographic conditions were as follows: the initial temperature was 50 or 120 °C for 0 min; it increased at a rate of 15 °C/min to 250 °C (15 min). The gas flow rate was 1.0 mL/min with helium used as a carrier gas. The amount of original compound and degraded materials were corrected with an internal control.

3.6 Measurement of intracellular PpIX

Cells (2×10^6 cells) were seeded in 6-cm dishes and incubated for 24 h. UTX-122 to UTX-128were added to the medium at the stated concentrations before ALA addition. After 4 h of incubation, cells were harvested using 2 mL of 0.25% Trypsin-1 mM EDTA. A cell suspension was collected in a 5-mL tube and centrifuged at 800 rpm for 5 min. The supernatant was removed with aspirator and cells were washed with phosphate-buffered saline. Finally, the cell pellet was suspended in 500 µL of 2.5% Triton X-100 solution and the cell suspension was transferred into a 0.5-mL micro tube, vortexed, incubated for 5 min at room temperature, and centrifuged at 15,000 rpm for 10 min. The fluorescence intensity of PpIX in the supernatant was measured using a SEC2000-UV/VIS spectrophotometer (excitation: 410 nm, emission: 630 nm).

4 Results

4.1 The enhancing effect of DCSA-based 4-alkylaniline derivatives on ALA-PDT

When the IC_{50} values of ALA in the ALA-PDT sensitive assay were evaluated, the combination treatment of DCSA and DCSA-based all 4-alkylaniline (C=0 to C=6) derivatives with ALA significantly enhanced the effect of ALA-PDT as compared with ALA alone (Fig. 16).
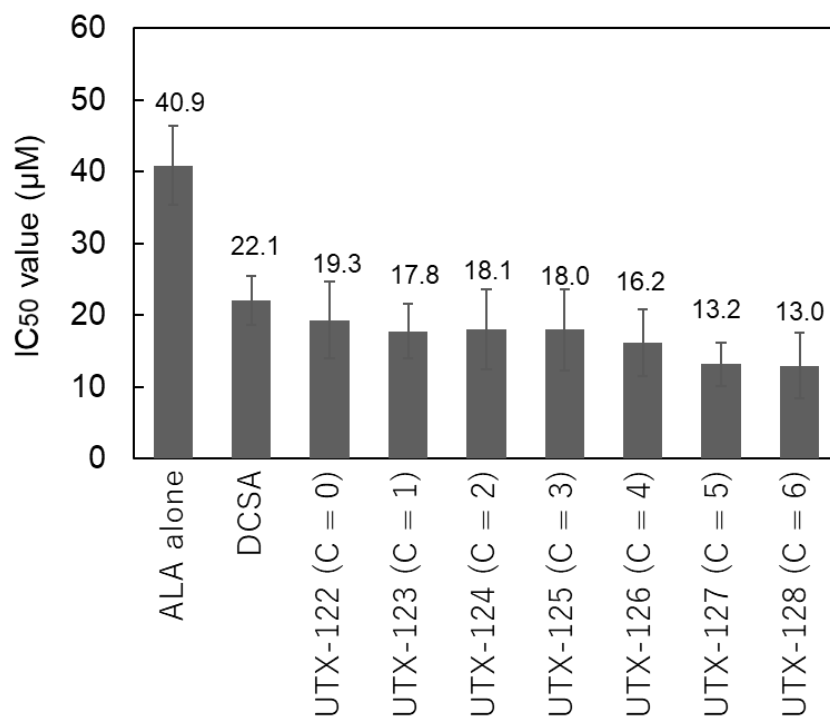

Fig. 16 Comparison of IC_{50} values in ALA-PDT sensitivity assay

4.2 DCSA-based 4-alkylaniline derivatives (C=4, C=5, C=6) are more stable in aqueous solution than TX-816

TX-816 is very unstable in an aqueous solution and quickly produced aldehyde and amine by hydrolysis (Fig. 17). Therefore, we examined the stability of the 4-alkylaniline derivatives using GC/MS system. In 10%-water/90%-DMSO solvent, TX-816 was rapidly hydrolyzed and > 50% of TX-816 was degraded within the first 5 min. After 70 min incubation, only 3.6% of the original TX-816 structure remained and almost the whole compound was converted into DCSA and CNA (54.4% and 42.0% respectively). On the other hand,

UTX-126 to UTX-128 were more stable than TX-816. After > 60 min incubation, DCSA-based derivatives were

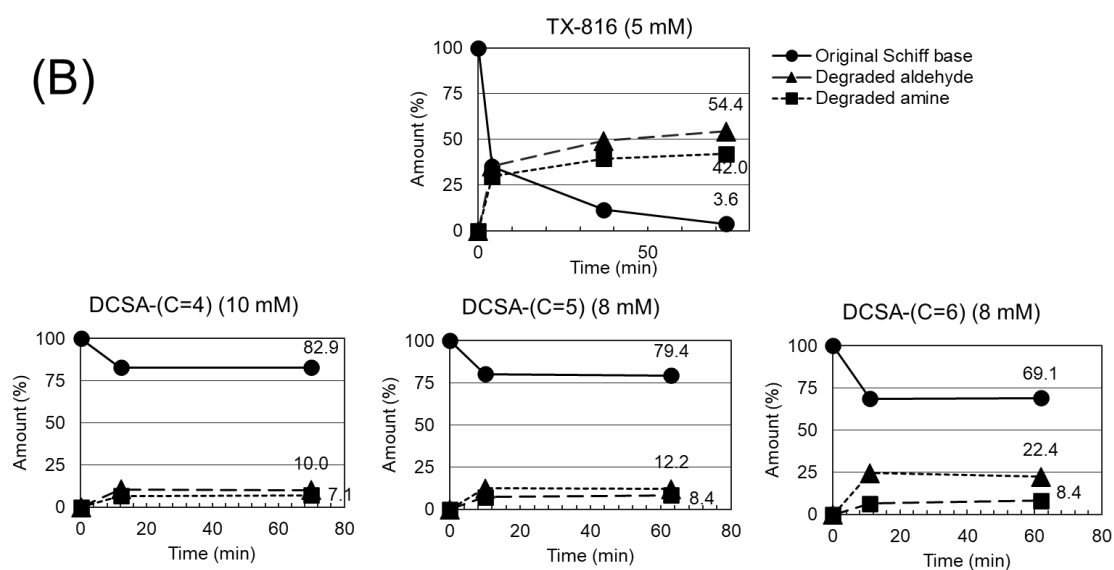maintained original structures (more than about 70%).
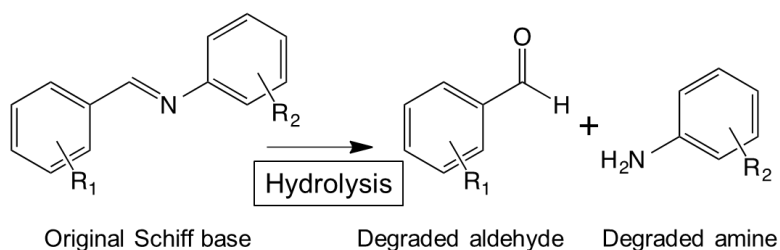
Fig. 17 Stability of Schiff base derivatives in 10% water / 90% DMSO solvent. Chemical structures of Schiff

base and its degradation products (A). Evaluation of stability by GC/MS analysis (B)

4.3 DCSA-based 4-alkylaniline derivatives increased an intracellular PpIX accumulation in MKN-45 cells

When MKN-45 cells were treated with 10 µM each compound and 50 µM ALA, the intracellular PpIX accumulation clearly increased in MKN-45 cells treated with DCSA-based derivatives as compared to those treated with the corresponding original compounds as shown in Fig. 18.
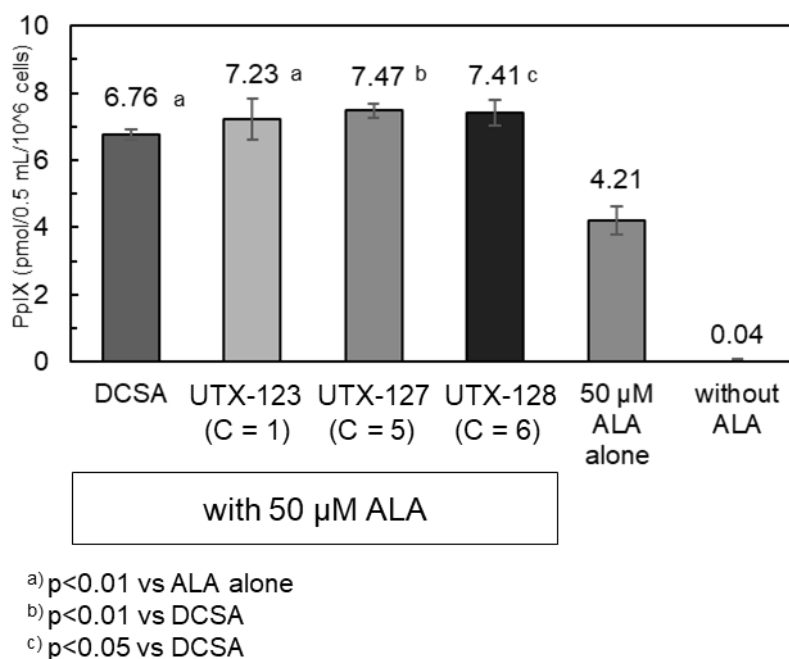

a) p<0.01 vs ALA alone
b) p<0.01 vs DCSA
c) p<0.05 vs DCSA

Fig.18 Increased intracellular accumulation of PpIX in MKN-45 after combination treatment with ALA and DCSA.

4.4 DSCA-based 4-alkylaniline derivatives were enhanced treatment effect to ALA-PDT resistance cells

UTX-127 and UTX-128 could effectively recover the sensitivity to ALA-PDT in R, R13 and R400 cells which are MKN-45 cells having acquired resistance (Fig.19). Their IC_{50} values of UTX-127 were 17.7 µM against MKN-45 cells, 226.4 µM against R cells, 378.3 µM against R13 cells and 335.1 µM against R400 cells, respectively. Their IC_{50} values of UTX-128 were 17.3 µM against MKN-45 cells, 379.9 µM against R cells and 198.0 µM against R400 cells, respectively. It demonstrated that these compounds were enhancing ALA-PDT effects to ALA-PDT resistance cells.

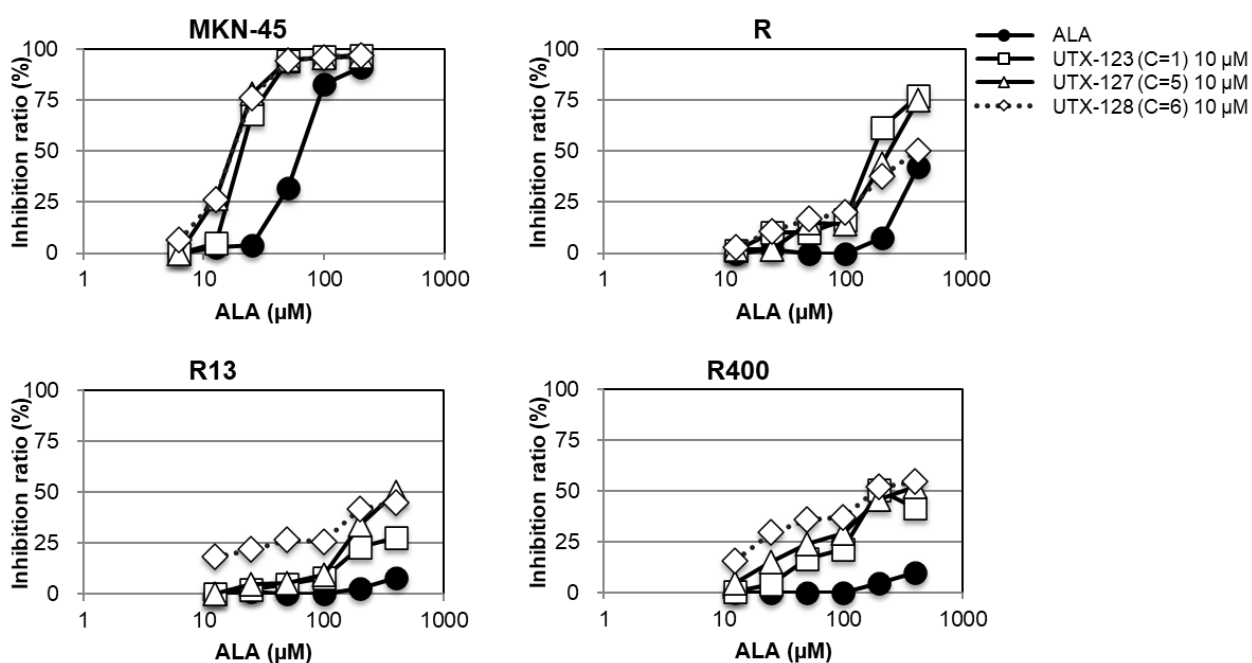DCSA derivatives (UTX-123, UTX-127 and UTX-128)

Fig.19 The ALA-PDT enhancing effects of Schiff base derivatives in parental MKN-45 cells and its ALA-PDT-resistant cell lines. Cells were seeded at a density of 5 x 10^3 cells/well in a 96-well plate. After 24 h of incubation, the compounds were added to the culture medium.

5. Discussion

In chapter 1, I found that the Schiff base derivative TX-816 significantly improved the sensitizing effect of ALA-PDT by significantly increasing the accumulation of intracellular PpIX. Although TX-816 was unstable in solvent by Schiff-base hydrolyzed [27,28], I synthesized new TX-816 derivatives with CNA substituted to 4-alkylaniline, which are much more stable than TX-816. The aldehyde group of DCSA is considered to have low stability in blood because it easily reacts with amines in serum proteins [30,31]. This chemical stability is thought to be taken up by tumor cells by retaining Schiff bases and then converted to DCSA.

UTX-126-128 were more stable than TX-816. Schiff-base compounds are generally hydrolyzed by undergoing a nucleophilic addition reaction on electron-deficient carbon. In TX-816, the imine carbon was electron-deficient by the NO_2 and Cl group of CNA known as electron-withdrawing group [29]. The improved stability of these compounds may be given by substitution of CNA with 4-alkylaniline possessing electron donating group. The imine carbon of Schiff-base structure in these DCSA-derivatives, UTX-126, UTX-127 and UTX-128, were obtained hydrolysis degradation resistant by substitution to alkyl-chain which is electron donating.

These derivatives were enhancing the cytotoxicity ALA-PDT against MKN-45 cells and resistant ALA-PDT cells, and increased accumulation of intracellular PpIX in MKN-45 cells. Although the ALA-PDT enhancing mechanism of these compounds is still unclear, it cannot rule out the possibility that the intact Schiff-base structure of DCSA-derivatives directly accelerate the cytotoxicity of ALA-PDT. It is suggested DCSA-derivatives maintaining the Schiff-base structure was taken up the cells and then they were partly hydrolyzed to generate DCSA in the cells. The DCSA or Schiff base compounds were maybe acted as iron chelating agents in the cells [32]. The chelated their compounds could down-regulated the levels of intracellular glutathione (GSH) which scavenges ROS generated from PpIX [33]. Therefore, it is considered the DCSA or its derivatives sensitized ALA-PDT.

6. Conclusion

In this chapter, UTX-122 to UTX-128 were improved the effect of ALA-PDT, and the sensitizing effect was tended to alkyl chain-dependent manner. UTX-126, UTX-127 and UTX-128 were more stable than TX-816, and their compounds were maintained original structures after >60 min incubation. UTX-127 and UTX-128 were increased the accumulation of intracellular PpIX as compared with ALA alone. UTX-127 and UTX-128 could effectively recover the sensitivity to ALA-PDT in ALA-PDT-resistance cells. It demonstrated that UTX-127 and UTX-128 showed higher stability to aqueous solution and stronger ALA-PDT-enhancing effect than DCSA, active body of TX-816.

References

[1] Shemin pathway and peroxidase deficiency in a fully habituated and fully heterotrophic non-organogenic sugarbeet callus: an adaptative strategy or the consequence of modified hormonal balances and sensitivities in these cancerous cells? A review and reassessment: T.Gaspar, C.Kevers, B.Bisbis, C.Penel, H.Greppin, F.Garnier, M.Rideau, C.Huault, J.P.Billard, J.M.Foidart, *Cell Prolif.,* 1999, 32, 249-270

[2] The Effect of Iron Ion on the Specificity of Photodynamic Therapy with 5-Aminolevulinic Acid: Hayashi M, Fukuhara H, Inoue K, Shuin T, Hagiya Y, Nakajima M, Tanaka T, Ogura S, *PLoS One,* 2015, 10, e0122351

[3] 5-Aminolevulinic acid (ALA) biosynthetic and metabolic pathways and its role in higher plants: a review: Yue Wu, Weibiao Liao, Mohammed Mujitaba Dawuda, Linli Hu, Jihua Yu, *Plant Growth Regulation*, 2019, 87, 357-374

[4] Monooxygenation of an Aromatic Ring by F43W/H64D/V68I Myoglobin Mutant and Hydrogen Peroxide: Thomas D. Pfister, Ohki T, Ueno T, Hara I, Adachi S, Makino Y, Ueyama N, Yi Lu, Watanabe Y, *J. Biol. Chem.* 2005, 280, 12858-12866

[5] Novel development of 5-aminolevurinic acid (ALA) in cancer diagnoses and therapy: Ishizuka M, Abe F, Sano Y, Takahashi K, Inoue K, Nakajima M, Kohda T, Komatsu N, Ogura S, Tanaka T, *Int. Immunopharmacol.*, 2011, 11, 358-365

[6] Haems and chlorophylls: comparison of function and formation: G.A.Hendry, O.T.Jones, *J.Med. Genet.*, 1980, 1-14

[7] The role of nitric oxide in δ-aminolevulinic acid (ALA)-induced photosensitivity of cancerous cells: Yamamoto F, Ohgari Y, Yamaki N, Kitajima S, Shimokawa O, Matsui H, Taketani S, *Biochem. Biophys. Res. Commun*, 2007, 353, 541-546

[8] Photodynamic Detection of Peritoneal Metastases Using 5-Aminolevulinic Acid (ALA).Yonemura Y, Endo Y, Canbay E, Liu Y, Ishibashi H, Mizumoto A, Hirano M, Imazato Y, Takao N, Ichinose M, Noguchi K, Li Y, Wakama S, Yamada K, Hatano K, Shintani H, Yoshitake H, Ogura SI. Cancers (Basel) 2017 Mar 1;9(3).

pii: E23. doi: 10.3390/cancers9030023. Review.

[9] Proton-coupled oligopeptide transporter family SLC15: physiological, pharmacological and pathological implications. Smith DE, Clémençon B, Hediger MA. Mol Aspects Med. 2013 Apr-Jun;34(2-3):323-36. doi: 10.1016/j.mam.2012.11.003. Review.

[10] Expression levels of PEPT1 and ABCG2 play key roles in 5-aminolevulinic acid (ALA)-induced tumor-specific protoporphyrin IX (PpIX) accumulation in bladder cancer. Hagiya Y, Fukuhara H, Matsumoto K, Endo Y, Nakajima M, Tanaka T, Okura I, Kurabayashi A, Furihata M, Inoue K, Shuin T, Ogura S. Photodiagnosis Photodyn Ther. 2013 Sep;10(3):288-95. doi: 10.1016/j.pdpdt.2013.02.001. Epub 2013 Mar 15.

[11] Pivotal roles of peptide transporter PEPT1 and ATP-binding cassette (ABC) transporter ABCG2 in 5-aminolevulinic acid (ALA)-based photocytotoxicity of gastric cancer cells in vitro. Hagiya Y, Endo Y, Yonemura Y, Takahashi K, Ishizuka M, Abe F, Tanaka T, Okura I, Nakajima M, Ishikawa T, Ogura S. Photodiagnosis Photodyn Ther. 2012 Sep;9(3):204-14. doi: 10.1016/j.pdpdt.2011.12.004. Epub 2012 Jan 4.

[12] The stem cell marker Bcrp/ABCG2 enhances hypoxic cell survival through interactions with heme: Partha Krishnamurthy, Douglas D. Ross, Takeo Nakanishi, Kim Bailey-Dell, Sheng Zhou, Kelly E. Mercer, Balazs Sarkadi, Brian P. Sorrentino, John D. Schuetz, *J. Biol. Chem.*, 2004, 279, 24218-24225

[13] The present and future role of photodynamictherapy in cancer treatmentStanley B Brown, Elizabeth A Brown, Ian Walker, *Lancet Oncol*, 2004, 5, 497-508

[14] Fluorescence-guided surgery with 5-aminolevulinic acid for resection of malignant glioma: a randomised controlled multicentre phase III trial: W. Stummer, U. Pichlmeier, T. Meinel, O. D. Wiestler, F. Zanella, H.J. Reulen, *Lancet Oncol*, 2006, 7, 392-401

[15] Expression of type-IV collagenases in human tumor cell lines that can form liver colonies in chick embryos. Tsuchiya Y, Endo Y, Sato H, Okada Y, Mai M, Sasaki T, Seiki M. Int J Cancer. 1994 Jan 2;56(1):46-51. DOI: 10.1002/ijc.2910560109.

[16] An overview of drug combination analysis with isobolograms. Tallarida RJ. J Pharmacol Exp Ther. 2006 Oct;319(1):1-7. doi: 10.1124/jpet.106.104117. Epub 2006 May 2.

[17] Identification of a mammalian mitochondrial porphyrin transporter. Krishnamurthy PC, Du GQ, Fukuda Y, Sun DX, Sampath J, Mercer KE, Wang J, Sosa-Pineda B, Murti KG, Schuetz JD. Nature 2006; 443:586-9. doi: 10.1038/nature05125.

[18] Human ABCB6 localizes to both the outer mitochondrial membrane and the plasma membrane. Paterson JK, Shukla S, Black CM, Tachiwada T, Garfield S, Wincovitch S, Ernst DN, Agadir A, Li X, Ambudkar SV, Szakacs G, Akiyama S, Gottesman MM. Biochem. 2007;46:9443-52. doi: 10.1021/bi700015m.

[19] Effects of plasma membrane ABCB6 on 5-aminolevulinic acid (ALA)-induced porphyrin accumulation in vitro: tumor cell response to hypoxia. Matsumoto K, Hagiya Y, Endo Y, Nakajima M, Ishizuka M, Tanaka T, Ogura S. Photodiagnosis Photodyn Ther. 2015 Mar;12(1):45-51. doi: 10.1016/j.pdpdt.2014.12.008.

[20] The influence of hypoxia and pH on aminolaevulinic acid-induced photodynamic therapy in bladder cancer cells in vitro. Wyld L, Reed MW, Brown NJ. Br J Cancer 1998;77:1621-1627.

[21] Hypoxia significantly reduces aminolevulinic acid-induced protoporphyrin IX synthesis in EMT6 cells. Georgakoudi I, Keng PC, Foster TH. Br J Cancer 1999;79:1372-1327. doi: 10.1038/sj.bjc.6690220.

[22] A perspective on efflux transport proteins in the liver. Köck K, Brouwer KL. Clin Pharmacol Ther. 2012 Nov;92(5):599-612. doi: 10.1038/clpt.2012.79. Epub 2012 Sep 5.

[23] The human ATP-binding cassette (ABC) transporter superfamily. Dean M, Hamon Y, Chimini G. J Lipid Res. 2001 Jul;42(7):1007-17. doi: 10.1101/gr.184901.

[24] The genetics of ATP-binding cassette transporters. Dean M. Methods Enzymol. 2005;400:409-29. doi: 10.1016/S0076-6879(05)00024-8.

[25] Development of a novel Schiff base derivative for enhancing the anticancer potential of 5-aminolevulinic acid-based photodynamic therapy, Shinohara Y., Endo Y., Abe C., Shiba I., Ishizuka M., Tanaka T., Yonemura Y., Ogura S., Tominaga M., Yamada H., Uto Y., Photodiagnosis Photodyn. Ther., 2017 Sep;(20):182-188. doi:10.1016/j.pdpdt.2017.10.014

[26] Improvement in titanium complexes supported by Schiff bases in ring-opening polymerization of cyclic esters: ONO-tridentate Schiff bases. Hsiu-Wei Ou, Wei-Yi Lu, Jaya Kishore Vandavasi, Ya-Fan Lin, Hsuan-Ying Chen, Chu-Chieh Lin, Polymer, 2018, 140, 315-325, doi: 10.1016/j.polymer.2018.02.016

[27] Unprecedented Water Effect as a Key Element in Salicyl-Glycine Schiff Base Synthesis: Karolina Bakalorz, Łukasz Przypis, Mateusz Michał Tomczyk, Maria Książek, Ryszard Grzesik, Nikodem Kuźnik, *Molecules*, 2020, 25, doi:10.3390/molecules25051257

[28] Stabilizing short-lived Schiff base derivatives of 5-aminouracils that activate mucosal-associated invariant T cells: Jeffrey Y. W. Mak, Weijun Xu, Robert C. Reid, Alexandra J. Corbett, Bronwyn S. Meehan, Huimeng Wang, Zhenjun Chen, Jamie Rossjohn, James McCluskey, Ligong Liu, David P. Fairlieb, *Nat. Commun.*, 2017, doi:10.1038/ncomms14599

[29] Reduction of nitro compounds carrying electron withdrawing groups: A convenient approach without metal catalyst: K. A.Vishnumurthy, A.V. Adhikari, *Chemica Date Collections*, 2019, 20, doi:10.1016/j.cdc.2019.100211

[30] Non-P450 aldehyde oxidizing enzymes: the aldehyde dehydrogenase superfamily: Satori A Marchitti, Chad Brocker, Dimitrios Stagos, Vasilis Vasiliou, *Exp Opin Drug Metab Toxicol*, 2008, 4, 697-720

[31] Novel and prevalent non-East Asian ALDH2 variants; Implications for global susceptibility to aldehydes' toxicity: Che-Hong Chen, Julio C.B.Ferreira, Amit U.Joshi, Matthew C.Stevens, Sin-JinLi, Jade H.-M.Hsu, Rory Maclean, Nikolas D. Ferreir, Pilar R.Cervantes, Diana D. Martinez, Fernando L. Barrientos, Gibran H. R. Quintanares, Daria Mochly-Rosen, *EBioMedicine*, 2020, 55, doi. 10.1016/j.ebiom.2020.102753

[32] The role of a Schiff base scaffold, N-(2-hydroxy acetophenone) glycinate-in overcoming multidrug resistance in cancer: Avishek Ganguly, Paramita Chakraborty, Kaushik Banerjee, Soumitra Kumar Choudhuri, Eur. J. Pharm. Sci. 2014, 51, 94-109, doi.org/10.1016/j.ejps.2013.09.003

[33] Dual-targeted 5-aminolevulinic acid derivatives with glutathione depletion function for enhanced photodynamic therapy: Ke Li, Wenyi Dong, Yinxing Miao, Qingzhu Liu, Ling Qiu, Jianguo Lin, J. Photochem. Photobiol. B, 2021, 215, doi.org/10.1016/j.jphotobiol.2020.112107